Structural, physicochemical characterization and antimicrobial activities of a new Tetraaqua bismaleato Iron(II) complex

BADIAA ESSGHAIER[a,*], JAWHER ABDELHAK[b], AMANI NAOUAR[a],
NOURCHENE TOUKEBRI[a], MOHAMED FAOUZI ZID[b] and NAJLA SADFI-ZOUAOUI[a]

[a]Laboratoire Microorganismes et Biomolécules Actives, Faculté des Sciences, 2092 El Manar, Tunis, Tunisie
[b]Laboratoire de Matériaux et Cristallochimie, Département de chimie, Faculté des Sciences,
2092 El Manar, Tunis, Tunisie
e-mail: badiaaessghaier@gmail.com; jawher.abdelhak@ipein.rnu.tn

Abstract. Tetraaqua bismaleato iron(II) $[Fe(C_4H_3O_4)_2(H_2O)_4]$, (**1**) is a new synthetic antimicrobial agent. Thermal analysis shows that the dehydration of the compound occurs in agreement with the structure. The single crystal salt crystallizes in the triclinic space group *P-1* with $a = 5.171(2)$ Å, $b = 7.309(3)$ Å, $c = 9.731(3)$ Å, $\alpha = 109.15(2)°$, $\beta = 115.02(2)°$, $\gamma = 92.42(1)°$, $V = 313.6(3)$ Å^3 and $Z = 1$. Three dimensional network is formed by strong intermolecular O – H . . . O hydrogen bonds. Magnetic susceptibility measurements of **1** in the range 2–300 K exhibited paramagnetic behavior at high temperature. However, at low temperature, the susceptibility data showed weak antiferromagnetic interactions between the local spins. Antimicrobial activity of **1** was tested. It showed high response against gram-positive and gram-negative bacteria as well as fungi and the MIC and IC50 values ranged from 8 to 256 μg.mL^{-1} and from 1.38 to 22.19 μg.mL^{-1}, respectively.

Keywords. Bismaleato complex; iron(II); single crystal; magnetic susceptibility; antibacterial; antifungal activities.

1. Introduction

The design and synthesis of complexes of carboxylic acids with transition metals are the most captivating studies in coordination chemistry and material science because of their interesting structures and spectroscopic, luminescence, catalytic, magnetic properties.[1–3] Metal complexes with maleate ligands have been recently investigated. They can form 1D, 2D or 3D networks and polynuclear complexes owing to the ligand coordination via O atoms and due to the formation of hydrogen bonds.[4]

This work is an extension of previous reports focused on frequently studied structures, $M^{II}(C_4H_3O_4)_2.4H_2O$, where M is Ni, Mn, Cd and Ba.[5,6] The purpose of the synthesis was to determine the metal ions effect on the coordination of maleato ion on the network of hydrogen bonds and the structural stability of these compounds. In this sense, our investigation has focused on the synthesis and characterization of a new species of the formula $[Fe(C_4H_3O_4)_2(H_2O)_4]$.

The need for new antimicrobial agents is greater than ever because of the emergence of multidrug resistance in common pathogens, the rapid emergence of

new infections, and the potential for use of multidrug-resistant agents.[7] Thus, there is a crucial requirement for the development of new classes of antimicrobial agents and the identification of new drug targets.[8] Several new approaches are required to combat emerging infections and the global spread of drug-resistant pathogens. These trends have emphasized the urgent need for new, more effective, less toxic and safe antimicrobial agents and the development of structurally new classes of antimicrobials with novel mechanisms of action to improve both their binding affinity and their spectrum of activity. Herein, we report the synthesis of a new antimicrobial agent designed tetraaqua bismaleato iron(II) and biological activities.

2. Experimental

2.1 *Materials and methods*

All chemicals were commercially purchased and used without further purification. TG/DTA 92 SETARAM thermal analyzer was employed for the investigation of the thermal behavior in Ar atmosphere from room temperature to 600°C. UV-Vis spectrum was recorded on a Perkin Elmer UV/Vis spectrometer Lambda 20

in the range 300-750 nm. Magnetic susceptibility measurements of a polycrystalline sample were carried out using a Quantum design (superconducting quantum interference device SQUID) magnetometer in the temperature range 2-300 K at a magnetic field of 200 G. The susceptibility data were corrected for diamagnetism estimated from Pascal's tables.[9]

Gram-negative bacterial strains of *Pseudomonas aeruginosa*, *Escherichia coli* DH5α *Acinetobacer spp*, *Agrobacteium tumefaciens* and *Erwinia* spp, gram-positive bacterial strains of *Listeria innocua, Staphylococcus aureus*, three yeasts *(Candida albicans)* and three fungal strains of dermatophyte*(Trichophyton rubrum)* were used in the present work. TSB and TSA media were employed throughout the experiments with bacteria. Yeast malt extract broth (YMB) and agar (YMA) were used in the test with *Candida albicans* and Potato Dextrose Agar (PDA) was used for experiments with fungi.

2.2 Synthesis

The title compound, tetraaqua bismaleato iron(II) (**1**) was prepared as good quality yellow single crystals from a mixture of iron(II) nitrate nanohydrate (0.3 g), maleic acid (0.4 g) and phosphoric acid (3 mL) dissolved in water (20 mL). The resulting mixture was heated to boiling point and stirred for two hours. Immediately a brown precipitate was formed. After a few days, single crystals were obtained by slow evaporation of an aqueous solution at room temperature. Anal. Found: C,16.02; H,1.73; Fe,12.25; O,24.54%; Calc. for $C_4H_{11}FeO_8$ (M.W. 363.09): C,16.3; H,1.62; Fe,12.1; O,25.31%.

2.3 Crystal structure determination and refinements

A prismatic red crystal ($0.22 \times 0.21 \times 0.13$ mm^3) was selected for the structural analysis. Diffraction data were collected at 293(2) K with Enraf–Nonius CAD4 automatic four-circle, equipped with a graphite monochromator using Mo K$_\alpha$ ($\lambda = 0.71073$ Å) radiation with the w-2θ technique. Unit cell parameters and orientation matrix of the crystal were determined by least squares treatment of the setting angles of 25 reflections on the range $10° < \theta < 15°$. The structure was solved by standard Patterson methods and refined by the full-matrix least-squares method on F^2 for 287 refined parameters. The structure was solved by direct methods and refined in a full-matrix anisotropic (isotropic for H) approximation using the SHELX-97 programs. The H atoms were located from difference Fourier syntheses

Table 1. Crystallographic and experimental data.

Formula	$C_4H_{11}FeO_8$
Formula weight (g.mol^{-1})	363.09
Crystal system	Triclinic
Space group	P-*1*
a (Å)	5.171(2)
b (Å)	7.309(3)
c (Å)	9.731(3)
α (°)	109.15(2)
β (°)	115.02(2)
γ (°)	92.42(1)
Volume (Å^3)	313.6(3)
Z	1
ρ (g.cm^{-3})	1.911
μ (mm^{-1})	1.61
Index ranges	$-1 \le h \le 6 ; -9 \le k$ $\le 9 ; -12 \le l \le 11$
Total data collected	1733
Independent reflections	1378
Reflections with I>2σ (I)	1336
R$_{int}$	0.0211
Goodness-of-fit on F^2	1.113
R [I>2σ(I)]^a	0.012
R$_w$ [I>2σ(I)]^b	0.049
Largest difference peak and hole (e Å^{-3})	0.53 and -0.45

^{a}R = $\Sigma ||F_0|-|F_c|| / \Sigma |F_0|$.
^{b}R$_w$ = $[\Sigma w(|F_0|^2|-F_c|^2)^2 / \Sigma w|F_0|^2]^{1/2}$

and refined as a rigid group. Further details of X-ray structural analysis are given in table 1.

2.4 Agar diffusion method

The *in vitro* antimicrobial test is based on the diffusion method on agar plates as previously reported.[10,11] Before use, **1** was diluted in distilled water, sterilized by filtration through a 0.2 μm pore size filter and adjusted to the appropriate concentration tested. A 50 μL aliquot of filtered compound was placed on paper discs. After overnight pre-diffusion at 4°C, the plates were incubated at appropriate temperature 37°C or 30°C for at least 24 h and diameters of inhibition zones were measured in mm.

2.5 Antifungal activity

2.5a *On PDA plates*: 50 μL of **1** at 200, 500 or 1000 μg.mL^{-1} were used to determine their efficiency on the growth dermatophyte inhibition by applying a dual culture technique as previously detailed.[11]

2.5b *In broth cultures of Candida albicans*: 100 μL of **1** at 200 μg.mL^{-1} was added to 900 μL of YM

medium containing 10^5 CFU of yeasts. The culture was then grown at 37°C on a shaker for 48 h, as previously detailed.[12]

2.6 *Determination of MIC and IC50*

The MIC (μg.mL^{-1}) was taken as the lowest concentration (highest dilution) without visible growth, and IC50 (μg.mL^{-1}) is the concentration at which 50% inhibition of the response is seen. MIC and IC50 value were evaluated by using the serial double dilution method in the appropriate medium which is inoculated with a standardized number of microorganisms. The concentration of **1** incubated with indicator strain is given in μg.mL^{-1}. Each dilution of **1** affected in 1000 μL of the appropriate medium was inoculated by 100 μL of 10^6 CFU mL^{-1} of each indicator strain then the different culture tubes were incubated at appropriate temperature. Control tube containing 100 μL of 10^6CFU.mL^{-1} of each indicator strain, added to 1000 μL of culture medium without **1**. MIC was estimated visually (absence of turbidity) and were determined with 3 independent measurements.[13]

2.7 *Determination of bactericide activity*

The antimicrobial activity of solutions of **1** was expressed in arbitrary units per mL (AU.mL^{-1}) and it was determined by an agar diffusion assay as previously described.[14] Briefly, a serial two-fold dilution in sterile distilled water of **1** was prepared, and 50 μL of each dilution were spotted onto a TSB agar soft plate seeded with about 10^5CFU.mL^{-1} of *Staphylococcus aureus*. The AU/mL was calculated as: AU/mL = 1000X D/A, where A is the volume of the **1** aliquot spotted on agar plate (50 μL in this case), D is the reciprocal of the highest dilution showing a clear inhibition of the indicator strain.

2.8 *Lysozyme activity*

The Lysozyme activity of the **1** was assayed turbidimetrically by measuring the decrease in absorbance at 660 nm of a suspension of *Staphylococcus. aureus*.[14]

2.9 *Mycelial hyphae destruction*

Fungal culture was rinsed with distilled sterile water. After centrifugation at 9000 rpm for 10 min pellet (mycelium) was replaced in an Eppendorf tube containing an appropriate Tris-HCl buffer (0,01 M, pH 8) in order to obtain the same concentration of mycelial solution (expressed in mg.mL^{-1}). 200 μL of 1000 μg.mL^{-1}

of the title compound was added. The mixture was incubated at 37°C for 14 h. Optical density was measured at 540 nm. Increase of OD was compared to control tube (containing only mycelial suspension) to make destruction of fungal hyphae by the compound.[15]

3. Results and Discussion

3.1 *Crystal structure description*

The title compound crystallized in the triclinic space group *P-1*. The Fe cations occupy inversion centers and the monodentate hydrogen maleate [$C_4H_3O_4$]$^-$ ligands are in a *trans* configuration (figure 1). The distorted octahedral iron coordination is completed by four water molecules, with Fe-O distances between 2.028(1) and 2.141(1) Å. The equatorial plane of the octahedron is formed by four oxygen atoms of water molecules (O2, O2^i) and anions maleato (O3 and O3^i) for the equation: 0,012(2) x − 2,881 (3) y + 4,487 (4) z = 5,441.

The elongation observed for M-O2 and M-O3 bonds with respect to M-O1 is probably due to the steric hindrance caused by the maleato groups which are quite bulky. Thereby, the maleato ion acts as a monodentate ligand bound by single oxygen. A maleic acid has a mirror-like symmetry perpendicular to the C2-C3 (table 2).

The distance C-C is between 1.23(3) Å and 1.32(3) Å, whereas the carbon - oxygen distance are of two types. The first category concerns the free oxygen atoms, where the distance C–O$_{free}$ is between 1.26(2) Å and
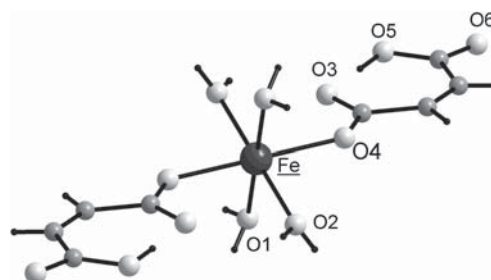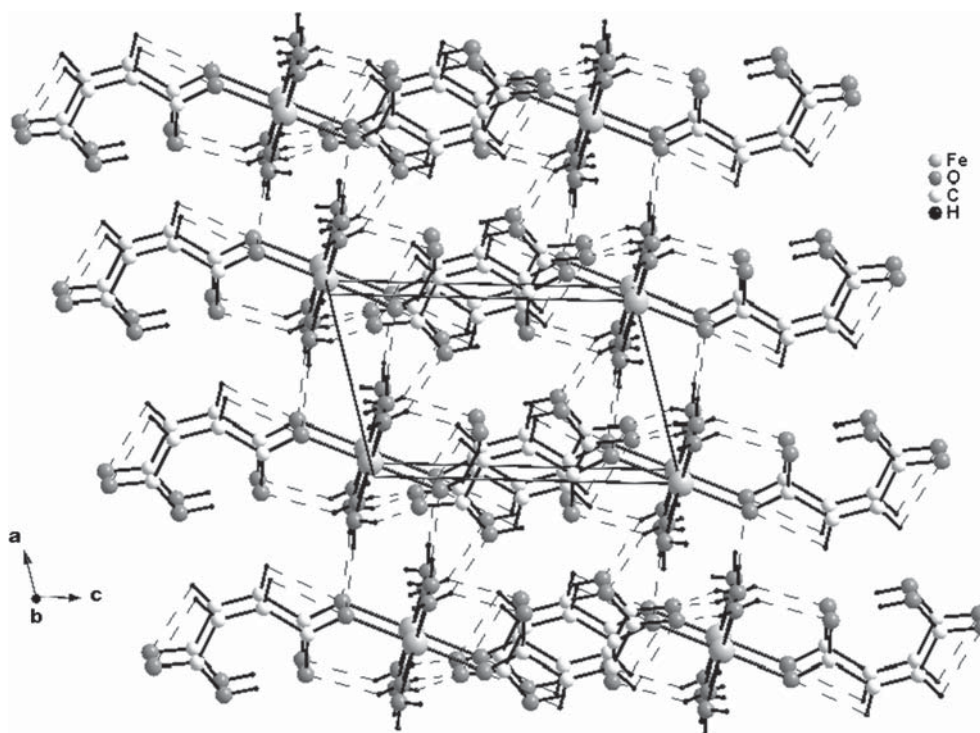

Figure 1. Molecular structure of [$Fe(C_4H_3O_4)_2(H_2O)_4$].

Table 2. Selected bond lengths (Å) and angles (°) in the octahedron FeO$_6$.

Fe – O1	2.028(1)	O1–**Fe** –O2	92.31(5)
Fe – O2	2.117(1)	O1–**Fe** –O3	84.31(1)
Fe – O3	2.141(1)	O2–**Fe** –O3	90.55(5)
		O1–**Fe** –O1^i	180.19(5)
		O2–**Fe** –O2^i	179.08(5)
		O3–**Fe** –O3^i	180.00(4)

Symmetry Code *i*: −x,−y,−z.

Figure 2. Fragments of the molecular structure showing directional hydrogen bonding interactions.

Table 3. Selected hydrogen–bond parameters for $[Fe(C_4H_3O_4)_2(H_2O)_4]$

D	H	A	D – H(Å)	H...A(Å)	D...A(Å)	D – H...A(°)
O2	H4	O3^{ii}	0.68(3)	2.13(4)	2.811(2)	178(4)
O2	H3	O6	0.82(3)	1.91(3)	2.725(2)	178(3)
O4	H5	O3^{iii}	0.86(5)	1.93(5)	2.777(2)	170(3)

D: donor; A: acceptor.
Codes of symmetry *ii:* -x,- y,−z+1 ; *iii:* x,- y+1,z-1.

1.29(3) Å, for the second category, oxygen atoms bound to metal ions, $d(C-O_{linked}) = 1.23(4)$ Å. These values are of the same order of magnitude as those reported.[16]

In the crystal structure, the molecules are packed via hydrogen bonds (figure 2) between water molecules and the uncoordinated O(maleate) atoms of neighboring molecules forming a two dimensional supramolecular structure (table 3).

3.2 *IR Spectra*

The infrared spectrum of compound $[Fe(C_4H_3O_4)_2(H_2O)_4]$ shows peaks relating to the maleate group. Asymmetric vibration modes of the CO bridge appear at 1630 cm^{-1}. The peak at 1365 may also be attributed to the symmetric vibration of C=O, so that the peaks in the vicinity of 750 cm^{-1} are assigned to the deformation vibration δ(OCO). The broad absorption band between 3500-2900 cm^{-1} can be attributed to OH and CH stretching vibrations. While peaks between 1250-600 cm^{-1} correspond to the carboxylic group deformations and δ(OH) vibrations. The peak at around 504 cm^{-1} is attributed to the stretching vibration ν(Fe-O). These allocations are in line with previous results.[17]

3.3 *Thermal analysis*

Thermal analysis was performed under a nitrogen atmosphere with a heating rate of 5°C.min^{-1} in a range between room temperature and 600°C. The TGA curve shows a mass loss corresponding to four water molecules (dehydration), this loss is reflected in the DTA curve with an endothermic peak at 177°C. In fact, the dehydration of the compound is in agreement with the structural study where we found that the cohesion between layers is ensured by strong hydrogen bonds between the water molecules and the maleate group of oxygen atoms. The percentage of the first loss of the mass is 22.72%, which is in agreement with the theoretical loss of four water molecules, 20.94 %. From 350°C, there is the decomposition of the organic group.

3.4 *Electronic Spectra*

Electronic absorption spectrum was obtained in ethanol solution. The absorption spectrum of the complex

shows very intense bands in the UV. For a Fe^{2+} ion with a d^6 configuration in an O_h crystal field and assuming a low-spin electronic configuration of complex, the $^1A_{1g}$ term is the ground state. Two lower energy transitions, $^1A_{1g} \rightarrow {}^1T_{1g}$ and $^1A_{1g} \rightarrow {}^1T_{2g}$ exhibit symmetry- and spin-forbidden character.[18,19] The peaks at 642 nm and 411 nm correspond to the two $t_{2g} \rightarrow e_g$ transitions. These represent, respectively, the $^1A_{1g} \rightarrow {}^1T_{1g}$ and $^1A_{1g} \rightarrow {}^1T_{2g}$ transitions.

3.5 *Magnetic Measurements*

The magnetic susceptibility data for polycrystalline samples of **1** were collected in the 2–300 K range, and the thermal variations of χ_m and χ_m^{-1} are shown in figure 3. It can be clearly seen that the sample is in a paramagnetic above 44 K. The plot of χ_m^{-1} versus temperature shows an exact linear relation at high temperature, which is well fitted by the Curie–Weiss equation, $\chi = C/(T-\theta)$, where C and θ are the Curie–Weiss constant and magnetic coupling parameter, respectively, to yield values for C and θ as, 3.37 cm^3.K.mol^{-1} and -1.88 K respectively. The highly negative θ value indicates dominant antiferromagnetic interactions.

An effective moment by formula unit can be extracted using the formula $\left(\frac{\mu_{eff}}{\mu_B}\right)^2 = \frac{3K_B C}{N}$.

Here, k_B is Boltzmann constant, C, Curie constant, N, the Avogadro's number, and μ_B, Bohr magneton. In the spin-only picture usually followed for localized spins of 3d ions, μ_{eff} is given by:

$\mu_{eff} = g\left[S\left(S+1\right)\right]^{1/2} \mu_B$, where g = 2.0 and S = 2 as usually observed for high-spin iron(II) complexes. The experimental value of μ_{eff} is higher than the theoretical spin-only value for Fe^{2+} $\left(\frac{\mu_{eff}}{\mu_B} = \sqrt{24} = 4.90\right)$.
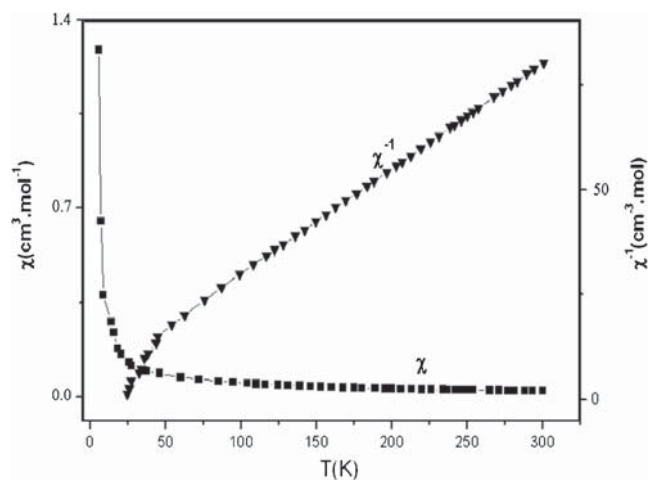
Figure 3. Thermal dependence of χ_m (■) and χ_m^{-1} (▶) for compound (**1**).

At room-temperature the magnetic moment of the compound is $\chi_m T = 3.59$ cm^{3}mol^{-1}.K, typical for HS iron(II). When the temperature decreases, the product value $\chi_m T$ gradually decreases until 2.36 cm^{3}mol^{-1} K. The local anisotropy of the metal ions (zero-field splitting effects) and/or intermolecular antiferromagnetic interactions of iron–iron would account for the observed decrease of $\chi_m T$ in the very low temperature domain causing the deviation from the Curie law.[20] To distinguish between these possibilities, we modeled the experimental data using a model that takes account of the ZFS parameter D in the equation of the molar magnetic susceptibility.[21]

$$\chi_m = \frac{Ng^2\mu_\beta^2}{3k_B T}\left(\chi_\parallel + 2\chi_\perp\right) \quad \text{with} \quad \chi_\parallel = \frac{1 + 9e^{\frac{-2D}{k_B T}}}{4\left(1 + e^{\frac{-2D}{k_B T}}\right)}$$

$$\text{and} \quad \chi_\perp = \frac{4 + \left(\frac{3k_B T}{D}\right)\left(1 + 9e^{\frac{-2D}{k_B T}}\right)}{4\left(1 + e^{\frac{-2D}{k_B T}}\right)}$$

Thus, it is concluded that the decrease was mainly due to $\chi_m T$ antiferromagnetic interactions that take place between the magnetic centers with very low or no contribution to ZFS. Therefore, based on these results, we can say that the field exerted by the ligands is weak (strong spin: HS). The refinement leads to a good agreement with the experimental $\chi_m T$ product for D = 6.10^{-3}cm^{-1} and TIP = 13.10^{-4}cm^3.mol^{-1}. This conclusion agrees well with the results of the X-ray structure determination showing that the shortest Fe-Fe distance exceeds 5 Å. It also suggests the absence of bridging ligands in this complex.

3.6 *Antimicrobial activity*

New antimicrobial agents are always needed to counteract the resistant pathogens that continue to be selected by current therapeutic regimens. In this context comes the objective of the present work to evaluate the antimicrobial potentialities of a new synthesized compound, tetraaqua bismaleato iron(II).

The antibacterial activities of the compound used at 100 μg.mL^{-1}, varied with the tested microorganisms; high activities were observed against *Pseudomonas aeruginosa, Escherchia coli* and *Acinetobacter spp* with a diameter of inhibition of, respectively, 15.5, 15 and 12 mm. Antifungal activity was also observed by **1** at 500 μg.mL^{-1} against species of *Candida albicans* with diameter inhibition of 14 mm. Noteworthy, that

1 was unable to inhibit fungi growth of the dermatophyte species used in this work by means of dual culture technique at the same concentration of 100 μg.mL^{-1}, neither by the application of 500 or 1000 μg.mL^{-1}.

On the whole, the results showed that **1** possesses high antibacterial activity at 100 μg.mL^{-1} compared to other published synthetic compounds.[22] At the highest concentration of about 500 μg.mL^{-1} of **1** also activity against *Candida albicans* strains has been obtained, similar to results obtained by synthetic compound reported.[22]

For antifungal activities numerous compounds had shown activity when applied with a concentration greater than 500 μg.mL^{-1}. In the present work, at 1000 μg.mL^{-1}, we have no antifungal activities in solid media compared to the antifungal activity exhibited by other synthetic compound.[22,23] For example, a number of methyl imidazole derivatives and some of their oxygenated products tested[23] were found to exert very low antifungal activity against yeasts and moulds.[23] The success of the application of Histidine-lysine (HK) polymers against the growth of several species of *Candida albicans* was described.[12]

In the light of the recently reported data, we decided to analyze the mechanism of action of the compound. For that, we have investigated the antifungal activities in broth medium for yeast and fungi. The results of the antifungal effect of **1** investigated in broth cultures of *Candida albicans* was determined as percent of yeast survival by measuring optical density at 600 nm. The obtained results showed that the application of **1** only at 200 μg.mL^{-1} was able to successfully suppress yeast survival by value ranging from 40.5 to 76.81 AU with various yeast strains tested in the present work, after incubation at 37°C for 48 h (figure 4).
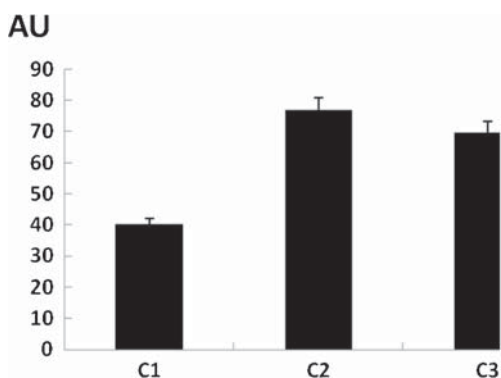
Figure 4. The effect of **1** at 200 μg.mL^{-1} on three strains of *Candida albicans,* C1, C2 and C3, tested by incubation for 14 h at 37°C. AU was expressed by comparison with untreated yeast suspension (incubation tube without **1**). Data are the average of three replications ± the standard error of the mean.

Previously, we have shown that the sulfanilamide sulphate used at 100 μg.mL^{-1} was able to suppress yeast survival only with 55.77 AU[11] and the aminochloropyridinium diaqua dioxalato iron(III) with value ranging from 45.45 to 24.53 AU.[24] These results show markedly high anti-*Candida* activities of the new compound described here with value 76.81 AU and 69.64 AU.

The values of MIC and IC50 are presented in table 4. The results have shown that MIC ranged from 8 μg.mL^{-1} for bacteria to 256 μg.mL^{-1} for yeast and IC50 values varying from 1.38 to 1.59 μg.mL^{-1} for bacteria and 22.19 for yeast. These results show that **1** had especially high activity against bacteria compared to yeast and fungi. Similar results of the promising antibacterial activities have been reported by two compounds[25] against *B. subtilis* with MIC of 1.12, 3.66 μg.mL^{-1}.

Our compound **1** has high antibacterial activities compared to a series of simple heterocyclic chalcone analogues described earlier,[26] which has moderate antibacterial activities since MIC exceed 32 μg.mL^{-1}.[26] Because of high antibacterial activities exhibited **1**, in the same context, we would evaluate their lysozyme and the bactericidal activities. The bactericide activity of **1** was expressed in arbitrary units per mL^{-1} (AU.mL^{-1}). The obtained results have shown that **1** had a high bactericidal activity of about 2500 AU.mL^{-1}. It should be mentioned that this value is greater than that exhibited by our previous compound di(4-sulfamoyl-phenyl-ammonium) sulphate.[11]

High lysozyme activities were expressed against *Listeria innocua* with 0.95 AU, greater than *Staphytococcus aureus* 0.087 AU. Lysozyme activities were directed toward membranes of gram-positive bacteria that are essentially constituted of peptidoglycans. Previously, similar high lysozyme activity against *Listeria innocua* was exhibited by other synthetic compounds as reported by our laboratory.[24]

The direct effect of the compound on mycelia growth gives an idea of the ability of the compound to

Table 4. MIC (μg.mL^{-1}) and IC50 values (μg.mL^{-1}) of Tetraaqua bismaleatofer(II) against pathogenic bacteria and yeast.

Microorganisms	MIC (in μg.mL^{-1})	IC50 (in μg.mL^{-1})
Bacteria		
Escherichia coli	8	1.38
Pseudomonas aeruginosa	8	1.59
Acinetobacter	8	1.5
Yeast		
Candida albicans	256	22.19

physically destruct the fungal hyphe. Markedly, the results of the investigation of the present compound showed that it was able to destruct the hyphe mycelial of three strains of the dermatophyte *Trichophyton rubrum* T1, T2 and T3 with values ranging from 0.057 to 0.632 AU. However, the high antifungal activities were obtained against T2 strain with 57% more than that for the strain T3 with 38%. The effect of **1** was markedly distinguished by the microscopic observation compared to untreated mycelium characterized by long hyphe (figure 5). It should be noted that **1** has high antifungal activities than our previous compound with activity not exceeding 0.1 AU against three tested dermatophyte strains.[24]

In previous work, we had shown the ability of di(4-sulfamoyl-phenyl-ammonium) sulphate to inhibit some phytopathogenic fungi by affecting the spores germination and mycelia fragmentation of fungi,[11] which could be useful in agriculture purposes. In this paper, the title compound was able to inhibit three strains of dermatophyte as well as three strains of *Candida albicans*. Based on the interest in antimicrobial activities, this new compound described here can be a promising antimicrobial agent.
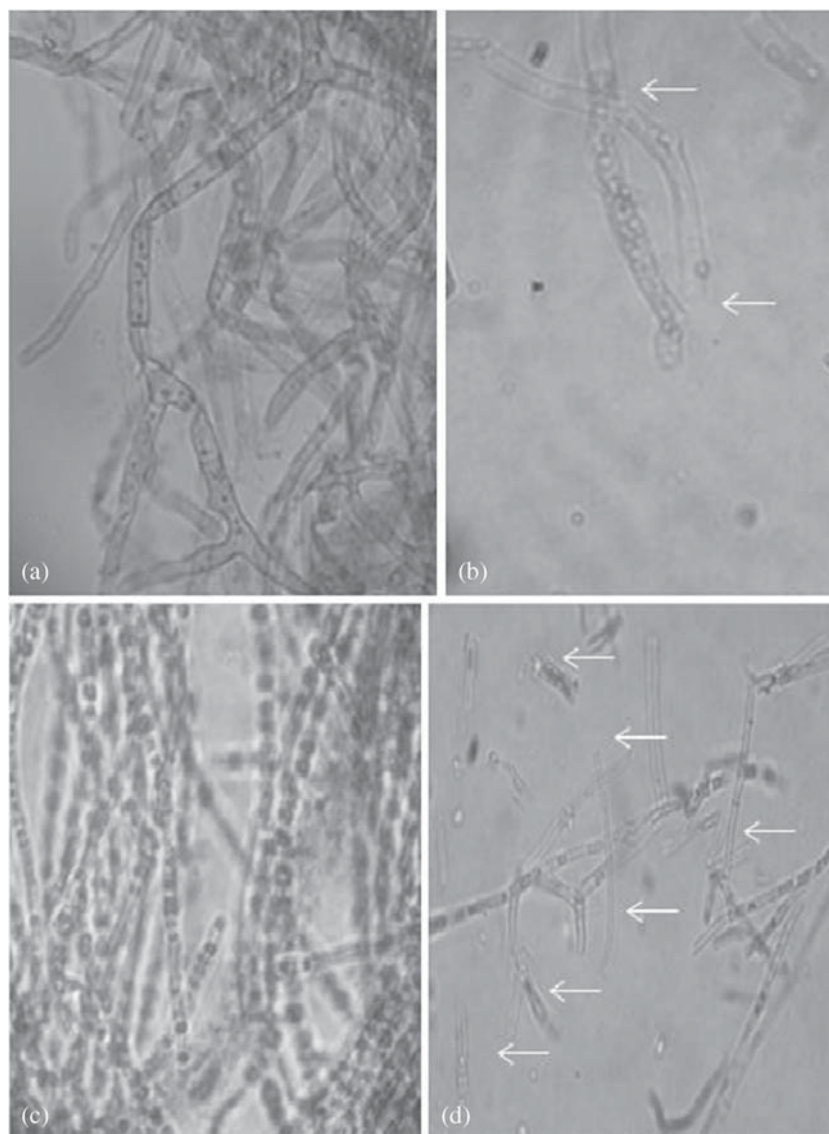
Figure 5. Microscopic observation of the effect of tetraaqua bismaleato iron(II) at 1000 μg.mL^{-1} on mycelial fragmentation of two strains T2 and T3 of *Trichophyton rubrum* (b) and (d), respectively; compared to untreated mycelial suspension (incubation tube without **1,** (a) and (c), respectively. Arrow indicates area of fragmentation and destruction hyphea compared to long hyphea in the normal case without treatment. Optical microscopic observation at 40X magnification.

4. Conclusions

In conclusion, the first part of the present work is a study of a new compound, tetraaqua bismaleato iron(II), containing maleate bridging ligand. The single-crystal X-ray data show elongated tetragonal-bipyramidal coordination around iron(II). The water molecules and oxygen for maleato anions are connected through hydrogen bonds into 3D supramolecular frameworks. Thermal analysis confirmed the number of water molecules as well as the nature of connections in the network of these molecules. These results are in perfect agreement with the structural study.

In the second part, the study has proved that the synthesized compound showed high antibacterial and antifungal activities against *Candida* and the dermatophyte strains. The results confirm that we have succeeded to synthesize a new compound more effective than our previous compounds published by our laboratory.[11,24]

Acknowledgements

Supplementary Information

Crystallographic data and full lists of bond lengths and angles have been deposited with the Cambridge Crystallographic Data Centre, CCDC No. 140005. Copies of this information may be obtained free of charge from The Director, CCDC, 12 Union Road, CAMBRIDGE CB2 1EZ, UK (fax: +44-1223-336-033; e-mail: deposit@ccdc.cam.ac.uk or **Error! Hyperlink reference not valid.** Additional two figures are available in Supplementary Information at www.ias.ac.in/chemsci.

References

1. Maspoch D, Ruiz-Molina D and Veciana J 2007 *Chem. Soc. Rev.* **36** 770
2. Sato O, Tao J and Zhang Y Z 2007 *Angew. Chem. Int. Ed.* **46** 2152
3. Kubota Y, Takata M, Kobayashi T and Kitagawa S 2007 *Coord. Chem. Rev.* **251** 2510
4. Smith C B, Barbour L J, Makha M, Raston L C and Sobolev A N 2006 *Chem. Commun.* 950
5. Zheng J L and Lin S K 2007 *Acta Cryst.* **E63** m1607
6. Liu Y 2005 *Acta Cryst.* **E61** m669
7. Spellberg B, Powers J H, Brass E P, Miller L G and Edwards J E 2004 *Clin. Infect. Dis.* **38** 1279
8. Waterman H, Tillen D and Dickson R 2001 *Health Technol. Assess.* **5** 1
9. Earnshaw A 1968 In *Introduction to Magnetochemistry* (London: Academic Press)
10. Collins M D, Facklam R R, Farrow J A E and Williamson R 1989 *FEMS Microbiol. Lett.* **57** 283
11. Essghaier B, Naouar A, Abdelhak J, Zid M F and Sadfi-Zouaoui N 2014 *Microbiol. Res.* **169** 504
12. Zhu J, Luther P W, Leng Q and Mixson A J 2006 *Antimicrob. Agents Chemother.* **50** 2797
13. Jorgensen J H and Turnidge J D 2007 *Am. Soc. Microbiol.* 1152
14. Graciela M, Vignolo M, De Kairuz N, Aida A P, De Ruiz H and Oilver G 1995 *J. Appl. Bacteriol.* **78** 5
15. Ryazanova L P, Stepnaya O A, Suzina N E and Kulaev I S 2005 *Process Biochem.* **40** 557
16. Kanters J A, Kroon J, Peerdeman A F and Schoone J C 1967 *Tetraheron* **23** 4027
17. Nakamoto K 2009 In *Infrared and Raman Spectra of Inorganic and Coordination Compounds Part B: Applications in Coordination, Organometallic, and Bioinorganic Chemistry* 6th ed. (Hoboken, New Jersey: John Wiley)
18. Lever A B P 1984 In *Inorganic Electronic Spectroscopy* 2nd ed. (Amsterdam: Elsevier) p. 212
19. Sabo T J, Grguric S R, Minic D M and Trifunovic S R 1998 *J. Coord. Chem.* **44** 47
20. Palamarciuc O V, Bourosh P N, Revenco M D, Lipkowski J, Simonov Y A and Clérac R 2010 *Inorg. Chim. Acta* **363** 2561
21. O'Connor C J 1986 *Prog. Inorg. Chem.* **29** 203
22. Abd El-Salam N M, Mostafa M S, Ahmed G A and Alothman O Y 2013 *J. Chem.* **2013** 1
23. Zani F P, Mazzal P, Benvenutiz S, Severi F, Malmusiz L, Vampa G and Antolin L 1995 *Eur. J. Med. Chem.* **30** 729
24. Abdelhak J, Essghaier B, Toukebri N, Naouar A, Rebib H, Zid M F and Sadfi-Zouaoui N 2014 *J. Microbiol. Biotech. Food* **4** 225
25. Sun J, Lv P C, Yin Y, Yuan R J, Ma J and Zhu H L 2013 *PLoS One* **8** e69751
26. Thanh-Dao T, Thi-Thao-Nhu N, Tuong-Ha D, Thi-NgocPhuong H, Cat-Dong T and Khac-Minh T 2012 *Molecules* **17** 6684